Stabilizing transglutaminase 2 in the open conformation results in reactive astrocytes being more neurosupportive.

Jacen Emerson[1]*, Thomas Delgado[1]*, Matthew Hong[1], Jeffrey W. Keillor[2] and Gail VW Johnson[1#]

[1]601 Elmwood Ave, box 604, Department of Anesthesiology and Perioperative Medicine, University of Rochester, Rochester, NY, 14620, USA
* These authors contributed equally to this work
[2] Department of Chemistry and Biomolecular Sciences, University of Ottawa, Ottawa, ON K1N6N5, Canada
[#]Corresponding author Gail_Johnsonvoll@urmc.rochester.edu

Abbreviations
CNS – Central nervous system
CSPG – Chondroitin sulfate proteoglycan
DIV – Days in vitro
ECM – Extracellular matrix
EV – Empty vector
H3K9ac – Acetylated histone H3 at lysine residue 9
HDAC – Histone de-acetylase
HEK293TN – Human embryonic kidney cells
IP – Immunoprecipitation
MAP2 – Microtubule-associated protein 2
PDL – Poly d-lysine
RNAPII – RNA polymerase II
SCI – Spinal cord injury
Sin3a – SIN3 transcription regulator family member A
TG2 – Transglutaminase 2
TG2-/- – Transglutaminase 2 knockout
WT – Wild type
Zbtb7a – Zinc finger and BTB domain containing 7a

Key Terms
TG2, Astrocytes, Neurosupportive phenotype, Histone modification

Abstract

Astrocytes play critical roles in supporting structural and metabolic homeostasis in the central nervous system (CNS). Inflammatory conditions bring about a range of poorly understood, heterogeneous, reactive phenotypes in astrocytes. Finding ways to manipulate the phenotype of reactive astrocytes, and leveraging a pro-recovery phenotype, holds promise in treating CNS injury. Previous studies have shown that the protein transglutaminase 2 (TG2) plays a significant role in determining the phenotype of reactive astrocytes. Recently it has been demonstrated that ablation of TG2 from astrocytes improves injury outcomes both *in vitro* and *in vivo*. Excitingly, in an *in vivo* mouse model, pharmacological inhibition of TG2 with the irreversible inhibitor VA4 phenocopies the neurosupportive effects of TG2 deletion in astrocytes. The focus of this study was to provide insights into the mechanisms by which TG2 deletion or inhibition of TG2 with VA4 result in a more neurosupportive astrocytic phenotype. Using a neuron-astrocyte co-culture model of neurite outgrowth, we show that VA4 treatment improves the ability of astrocytes to support neurite outgrowth on an injury-relevant matrix, further validating the ability of VA4 to phenocopy astrocytic TG2 deletion. VA4 treatment of neurons alone had no effect on neurite outgrowth. VA4 covalently binds to active site residues of TG2 that are exposed in its open conformation and are critical for its enzymatic function, and prevents TG2 from taking on a closed conformation, which interferes with its protein scaffolding function. To begin to understand how pharmacologically altering TG2's conformation affects its ability to regulate reactive astrocyte phenotypes, we assayed the impact of VA4 on TG2's interaction with Zbtb7a, a transcription factor that we have previously identified as a TG2 interactor, and whose functional outputs are significantly regulated by TG2. The results of these studies demonstrated that VA4 significantly decreases the interaction of TG2 and Zbtb7a. Further, previous findings indicate that TG2 may act as an epigenetic regulator, through its nuclear protein-protein interactions, to modulate gene expression. Since both TG2 and Zbtb7a interact with members of the Sin3a chromatin repressor complex, we assayed the effect of TG2 deletion and VA4 treatment on histone acetylation and found significantly greater acetylation with TG2 deletion or inhibition with VA4. Overall, this work points toward a possible epigenetic mechanism by which genetic deletion or acute inhibition of TG2 leads to enhanced astrocytic support of neurons.

Introduction

Astrocytes are unique and versatile cells of the central nervous system (CNS). In homeostatic conditions, astrocytes maintain the blood-brain barrier, regulate the extracellular matrix (ECM), and provide crucial metabolic support for neurons, among other functions (Sofroniew and Vinters 2010, Chung *et al.* 2015, Barres 2008). Inflammatory and stress signals, whether from injury, infection, or other sources, cause astrocytes to take on a range of phenotypes from neuroprotective to neurotoxic, although the exact molecular determinants of these phenotypes are poorly understood (Anderson *et al.* 2014, Burda *et al.* 2022, Escartin *et al.* 2021, Linnerbauer and Rothhammer 2020, Davies *et al.* 1997, Guttenplan *et al.* 2021, Liddelow *et al.* 2017, Smith and Strunz 2005, Yiu and He 2006). Previously, our lab has implicated the protein transglutaminase 2 (TG2) as a key factor in modulating the phenotype of reactive

astrocytes (Colak and Johnson 2012, Elahi *et al.* 2021, Emerson *et al.* 2023, Feola *et al.* 2017, Monteagudo *et al.* 2018).

TG2 is a widely expressed, multi-functional protein in the transglutaminase family, and is the transglutaminase with the highest expression in the brain. TG2 has been studied mostly as an enzyme that catalyzes the incorporation of an amine into a glutamine of the acceptor protein (Gundemir *et al.* 2012, Griffin *et al.* 2002, Chen and Mehta 1999, Farrelly *et al.* 2019, Lepack *et al.* 2020). This reaction requires calcium which stabilizes TG2 in this catalytically active, open conformation (Keillor and Johnson 2021, Pinkas *et al.* 2007). Conversely, GTP/GDP stabilizes TG2 in the closed, catalytically inactive conformation, and due to the relatively high concentrations of intracellular GTP/GDP to calcium, in basal conditions TG2 is predominantly in its catalytically inactive form (Begg *et al.* 2006, Liu *et al.* 2002). Additionally, in the closed conformation, TG2 can function as a scaffold for protein-protein interactions at the cell surface and in the nucleus, with well-described roles, for example, in cell-ECM interactions and chromatin regulation (Chen and Mehta 1999, Gundemir et al. 2012, Akimov and Belkin 2001, Begg et al. 2006, Farrelly et al. 2019, Eckert *et al.* 2014, Rossin *et al.* 2023, van Strien *et al.* 2011a). In response to injury, TG2 expression is often increased as its expression is regulated by transcription factors associated with inflammation and hypoxia (Filiano *et al.* 2010, Ientile *et al.* 2004, Ientile *et al.* 2015).

Previously we have described the role of astrocytic TG2 in different injury models. Depletion of astrocytic TG2 makes astrocytes more resilient to oxygen-glucose deprivation and improves their ability to protect neurons from such conditions (Colak and Johnson 2012, Monteagudo et al. 2018, Quinn *et al.* 2018). *In vivo*, mice with TG2 selectively knocked out of astrocytes showed significantly faster motor recovery after spinal cord injury (SCI) compared to wild type (WT) mice (Elahi et al. 2021). Following this intriguing finding, we used a chondroitin sulfate proteoglycan (CSPG) inhibitory matrix to simulate the growth-inhibitory environment of the spinal cord lesion core *in vitro* in order to investigate possible mechanisms by which TG2 knockout (TG2-/-) astrocytes promote greater functional recovery after SCI. We found that these astrocytes facilitated neurite outgrowth across the simulated injury matrix to a greater extent than WT astrocytes (Emerson et al. 2023). These studies demonstrate that deletion of TG2 from astrocytes significantly increases their ability to support neurite outgrowth on a growth-inhibitory matrix and neuronal regeneration after injury. The molecular mechanisms that underlie these enhanced neurosupportive functions of TG2-/- astrocytes have yet to be identified.

To complement the studies on how TG2 deletion impacts the ability of astrocytes to be neurosupportive, we have examined the effects of pharmacologically inhibiting TG2 using VA4. VA4 irreversibly inhibits TG2 function by binding to active site residues necessary for its catalytic activity, “locking” TG2 in its open conformation, thereby also preventing protein scaffolding function associated with its closed conformation (Gundemir *et al.* 2017, Mironov *et al.* 2016, Keillor and Johnson 2021, Liu et al. 2002). Previously we demonstrated that VA4 treatment of WT astrocytes phenocopied many of the functional effects of TG2 depletion: (1) VA4 treatment of WT astrocytes significantly improves survival after an ischemic insult (Feola et al. 2017), and (2), *in vivo*, VA4 treatment of WT mice significantly improved functional recovery after SCI, compared to vehicle treatment, to an extent similar to that observed in mice with astrocyte specific TG2 deletion. (Elahi et al. 2021). These data indicate that VA4 has the potential to promote neurosupportive phenotypes in reactive astrocytes after CNS injury. The

focus of this present study was to extend our mechanistic understanding of the neurosupportive effect of astrocytic TG2 depletion and inhibition.

Results

VA4 Neurite Outgrowth

Previously, we demonstrated that VA4 inhibition of TG2 phenocopies the neurosupportive effects of astrocytic TG2 deletion in a SCI model and *in vitro* using an ischemia-reperfusion model (Elahi et al. 2021, Feola et al. 2017). In the past we used an *in vitro* neurite outgrowth model where WT or TG2-/- astrocytes were grown on transwells and paired with neurons seeded on a growth-supportive poly-D-lysine (PDL) matrix or an injury-relevant, growth-inhibitory matrix comprised of CSPGs. Compared to WT astrocytes, TG2-/- astrocytes promoted significantly greater neurite outgrowth on the inhibitory CSPG matrix (Emerson et al. 2023), although neither WT nor TG2-/- astrocytes were able to increase neurite complexity (Fig. S1). To determine the effect of VA4 treatment on the ability of WT astrocytes to support neurite outgrowth, WT astrocytes were incubated with or without VA4, and then paired, with neurons grown on an inhibitory CSPG matrix. Figure 1a illustrates the paradigm. As expected, the presence of astrocytes resulted in significantly greater neurite outgrowth on CSPGs compared to unpaired neurons. Similar to the enhanced neurite outgrowth observed in the presence of TG2-/- astrocytes (Emerson et al. 2023), neurons paired with VA4-treated astrocytes promoted significantly greater neurite outgrowth compared to vehicle-treated astrocytes (Fig. 2b,c). Importantly, VA4 treatment of neurons alone did not affect their neurite outgrowth on a PDL or CSPG matrix (Fig. S2).

Immunoprecipitation of TG2 and Zbtb7a after VA4 Treatment

The ability of TG2 to regulate gene expression has been well described in the literature; however, the mechanisms by which it does so, and the functionally significant genes impacted in astrocytes have not been fully delineated (Gundemir et al. 2012, Eckert et al. 2014, Kim *et al.* 2021, Tatsukawa *et al.* 2016). Nuclear fractionation has shown that TG2 is enriched in the chromatin fraction (Lesort *et al.* 1998). IT exhibits a functionally significant interaction with the transcription factor-like protein Zbtb7a, which regulates gene expression in part by altering promoter accessibility (Emerson et al. 2023, Pittol *et al.* 2018). To interrogate how VA4 may alter the interaction of TG2 with Zbtb7a, and thus gene expression, HEK cells were transfected with V5-tagged TG2 and FLAG-tagged Zbtb7a, followed by VA4 or vehicle-only treatment and subsequent analysis of TG2-Zbtb7a interactions (Emerson et al. 2023). Immunoprecipitation (IP) of TG2 from the VA4-treated cells resulted in significantly less pull down of Zbtb7a compared to vehicle-only treated cells (Fig. 2).

Histone Acetylation in WT and TG2-/- Astrocytes

TG2 and Zbtb7a both interact with components of Sin3a, a transcriptional repressor complex that facilitates chromatin modifications by HDAC1 and HDAC2 (Emerson et al. 2023, Laudes *et al.* 2008). Considering this and the predominant upregulation of gene expression when TG2 is deleted (Elahi et al. 2021, Monteagudo et al. 2018), we hypothesized that TG2 limits the chromatin accessibility of reactive astrocytes in part through regulating histone

acetylation. Acetylated H3K9 (H3K9ac) localizes to active gene promoters and is associated with enhanced transcriptional activity (Gates *et al.* 2017). Therefore, we measured H3K9ac levels in WT and TG2-/- astrocytes and found that the levels in TG2-/- astrocytes are significantly higher than in WT astrocytes (Fig. 3).

Histone Acetylation after VA4 Treatment in WT Astrocytes

Given the significantly higher levels of H3K9ac in TG2-/- astrocytes, we asked whether VA4 treatment of WT astrocytes could replicate this epigenetic effect. WT astrocytes were treated with 10 µM VA4 for 48 hours prior to analysis. These data demonstrate that VA4-treated astrocytes exhibit a significant increase in H3K9ac levels compared to vehicle treated astrocytes (Fig. 4), comparable to the levels observed in TG2-/- astrocytes (Fig. 3).

Discussion

There is growing evidence that TG2 plays a significant role in regulating the phenotype of reactive astrocytes (Espitia Pinzon *et al.* 2017, van Strien *et al.* 2011b, Colak and Johnson 2012, Elahi et al. 2021, Emerson et al. 2023, Feola et al. 2017, Monteagudo et al. 2018, Delgado and Johnson 2024). In different injury models, it has been demonstrated that deletion or depletion of TG2 from astrocytes enhances their ability to support neuronal viability and recovery after injury compared to controls (Colak and Johnson 2012, Elahi et al. 2021, Emerson et al. 2023, Monteagudo et al. 2018). Most notably, mice with astrocyte-specific TG2 deletion recover motor function significantly faster and to an overall greater extent after SCI compared to WT mice. To further investigate this finding, we recently used a transwell astrocyte-neuron co-culture design to show that TG2-/- astrocytes better support neurite outgrowth on an injury-relevant, growth-inhibitory matrix. The implications and limitations of this finding were discussed in depth in the previous paper; chiefly, this data suggests that enhanced axonal regeneration is a possible mechanism underlying the improved motor function recovery after SCI in astrocytic TG2-/- mice (Emerson et al. 2023). Here we follow up on another finding from our SCI model — treatment of mice with the irreversible TG2 inhibitor, VA4, phenocopied the effects of astrocytic specific TG2 deletion, i.e., a significantly faster and greater extent of functional recovery compared to vehicle only treated mice (Elahi et al. 2021). These findings complemented our prior findings that VA4 treatment improved astrocyte survival in *in vitro* injury model systems (Feola et al. 2017, Elahi et al. 2021). Herein, we demonstrate that treatment of astrocytes with VA4 significantly increases their ability to promote neurite outgrowth on a growth-inhibitory matrix, thus further phenocopying the effects of astrocytic TG2 depletion.

To begin to elucidate the mechanisms underlying the effects of VA4 treatment, we tested whether VA4 modulates the interaction of TG2 and Zbtb7a, a transcription factor that we previously identified as a TG2 interactor (Emerson et al. 2023). Based on results of our IP experiments, and the established roles of TG2 for regulating gene expression (Elahi et al. 2021, Feola et al. 2017, Filiano *et al.* 2008, Gundemir *et al.* 2013, Kim et al. 2021, McConoughey *et al.* 2010, Monteagudo et al. 2018, Rossin et al. 2023), and Zbtb7a for regulating chromatin accessibility (Pittol et al. 2018, Monteagudo et al. 2018), we hypothesized that TG2 binds with transcription factors such as Zbtb7a to influence chromatin accessibility in astrocytes. In line with this hypothesis, VA4 significantly decreases TG2 binding to Zbtbt7a. Further, TG2 may also

associate with and influence chromatin regulatory complexes. Interestingly, both TG2 (Emerson et al. 2023) and Zbtb7a (Choi *et al.* 2009) can bind to proteins within the Sin3a complex, a transcriptional repressor complex important for gene regulation in response to environmental stress (Tiana *et al.* 2018). Sin3a complex proteins associate with the histone deacetylases HDAC1 and HDAC2 to decrease chromatin accessibility (Kadamb *et al.* 2013). Therefore, we measured acetylated histone levels, markers of chromatin accessibility and gene transcription, in WT and TG2-/- astrocytes. For these studies, we specifically measured the levels of H3K9ac, as this histone modification is well-established as a mediator of increased chromatin accessibility and transcriptional activity (Gates et al. 2017). Both TG2 deletion and VA4 treatment significantly increased the level of H3K9ac in astrocytes. These findings are in agreement with previous results showing gene upregulations in injured spinal cord tissue from mice with astrocytic TG2 deletion and cultured TG2-/- astrocytes (Monteagudo et al. 2018, Elahi et al. 2021).

TG2 is an injury-responsive protein whose function depends on many factors, including cellular localization. While TG2 is predominantly cytosolic, it migrates in and out of the nucleus (depending on cell type) in response to injury to influence gene expression (Gundemir et al. 2013, Gundemir and Johnson 2009, Ji *et al.* 2018, Quinn et al. 2018, Yunes-Medina *et al.* 2017). Our lab and others have shown that TG2's regulation of gene expression can be mediated through its ability to act as a protein scaffold, in which it may bring together transcription factors and chromatin regulatory complexes (Basso and Ratan 2013, Colak *et al.* 2011, Farrelly et al. 2019, Filiano et al. 2008, Gundemir et al. 2013, Gundemir and Johnson 2009, Lepack et al. 2020, McConoughey et al. 2010, Milakovic *et al.* 2004, Rossin et al. 2023, Rroji *et al.* 2021). In astrocytes, TG2 is strongly associated with transcriptional repression, and, given the aforementioned effects of astrocytic TG2 depletion, we hypothesize that nuclear TG2 attenuates the upregulation of neurosupportive signaling pathways in astrocytes during stress. In line with this hypothesis, inhibition of astrocytic TG2 function by VA4 replicates the neurosupportive effects of TG2-/- astrocytes. VA4 binds to TG2's catalytic domain and blocks TG2's catalytic activity and locks TG2 in the open conformation, preventing potential scaffolding interactions dependent on its closed conformation (Keillor and Johnson 2021). VA4 therefore putatively limits TG2's ability to interact with nuclear proteins, which we confirmed for Zbtb7a. Interestingly, however, previous data from our lab using overexpression constructs of mutant TG2 with deficient catalytic and GTP-binding ability may suggest that TG2 can still regulate gene expression in the open conformation, independent of its catalytic activity (Gundemir and Johnson 2009). To what degree TG2's open and closed conformations contribute to its ability to bind to and scaffold between nuclear proteins, and more specifically, which protein domains are important for these interactions remain open questions. The ability of VA4-treated astrocytes to phenocopy TG2-/- astrocytes suggests that protein scaffolding mediated by TG2 in the closed conformation plays a pivotal role in the functional differences between WT and TG2-/- astrocytes. However, further work is needed to determine whether VA4 alters TG2 translocation to the nucleus, which could alternatively lead to transcriptional and functional changes associated with TG2 deletion. Further work also needs to be done to determine the relative contributions of TG2's ability to catalytically modify nuclear proteins and TG2's nuclear scaffolding function to its overall effect in astrocytes of upregulating neurosupportive function in response to stress (Rossin et al. 2023, Basso and Ratan 2013, Farrelly et al. 2019).

The TG2-Zbtb7a-Sin3a interaction represents a potentially important mechanism for how TG2 regulates gene expression in response to stress (Emerson et al. 2023, Laudes et al. 2008). The Sin3a complex is an important regulator of gene expression during stress, particularly in hypoxic stress (Yunes-Medina et al. 2017, Tiana et al. 2018, Icardi *et al.* 2012). Indeed, it regulates the vast majority of the transcriptional response to hypoxia and is necessary for a complete response (Tiana et al. 2018). Our data suggests that TG2 facilitates histone deacetylation, but as TG2 lacks a canonical DNA binding motif, this effect is likely mediated through TG2 partnering with DNA-binding transcription factors, like Zbtb7a, and with proteins capable of recruiting a histone de-acetylase, like members of the Sin3a complex. Figure 5 summarizes the proposed mechanism by which TG2 may mediate the neurosupportive status of reactive astrocytes. Considering that TG2 is able to interact with a range of stress-responsive transcription factors, including Rb, HIF1β, and NF-κB (Feola et al. 2017, Filiano et al. 2008, Milakovic et al. 2004), we will need to determine the relative contribution of TG2-Zbtb7a-Sin3a interactions to TG2's ability to regulate gene expression in response to stress (Eckert et al. 2014). Figure 5 summarizes the proposed mechanisms by which TG2 may regulate gene expression in astrocytes.

Methods and Materials

Animals

All mice and rats were maintained on a 12 hour light/dark cycle with food and water available ad libitum. The procedures with animals were in accordance with guidelines established by the University of Rochester Committee on Animal Resources. The studies were carried out with approval from the Institutional Animal Care and Use Committee. WT C57BL/6 mice were originally purchased from Charles River Laboratories. TG2-/- mice on a C57Bl/6 background were described previously and have been continuously bred in house since (Colak and Johnson 2012). Timed pregnant Sprague Dawley rats were obtained from Charles River Laboratories.

Cell Culture

Primary astrocytes were cultured at post-natal day 0 from either WT C57BL/6 or TG2-/- mouse pups as previously described (Colak and Johnson 2012). In brief, post-natal day 0 mouse pups were rapidly decapitated, the brains were collected and dissected, meninges removed, and cortical hemispheres were collected. Following trituration of the cells, they were plated onto culture dishes in MEM supplemented with 10% FBS (Atlas Biologicals, F-0500-DR) 33 mM glucose, 1mM sodium pyruvate (Gibco, 11360-070), and 0.2% Primocin (Invivogen ant-pm-05) (glial MEM). Twenty-four hours later, the dishes were shaken vigorously and rinsed to remove debris and other cell types. Astrocytes were maintained at 37°C/5% CO_2 for 7-8 days, frozen in glial MEM containing 10% DMSO, and stored in liquid nitrogen. For experiments, astrocytes were thawed and grown to confluency in glial MEM. The cells were passaged, and then used for all the studies.

Primary cortical neurons were prepared from Sprague Dawley rat embryos at embryonic day 18 (E18) and cultured as previously described with some modifications (Ji et al. 2018). To prepare the coverslips/wells, poly-D-lysine (Sigma P6407) was diluted in PBS to a concentration of 20

µg/mL and added to the wells for 4 h. The wells were either rinsed and stored with PBS, or after rinsing, CSPGs (Millipore, CC117) in PBS (2.5 µg/mL) were added and incubated overnight to coat the coverslips. All wells and coverslips were rinsed with PBS prior to plating the neurons. To prepare the neurons, a pregnant rat was euthanized using CO_2, followed by rapid decapitation in accordance with NIH Animal Research Advisory Committee guidelines. Embryos were removed, rapidly decapitated, brains were extracted, cerebral cortices dissected, and meninges were removed. Cerebral cortices were then digested in trypsin-EDTA (0.05%) (Corning, 25-053-Cl) for 15-20 min in a 37°C water bath. Following gentle trituration, neurons were plated in neuron plating medium consisting of MEM (Gibco, 42360032) supplemented with 5% FBS, 20 mM glucose, and 0.2% Primocin to a density of 12,000 cells/cm^2 on the coated coverslips. Four to five hours later, the medium was replaced with Neurobasal medium (Gibco, 21103-049) containing 2% B27 (Gibco, 17504-044), 0.5mM Glutamax (Gibco, 35050-061) and 0.2% Primocin (neuron growth medium). Neurons were incubated at 37°C/5% CO_2 and experiments begun at days in vitro (DIV) 1.

HEK293TN cells were thawed and grown at 37°C/5% CO_2 in DMEM (Gibco 11995-065) supplemented with 10% FBS, 1x GlutaMAX (Gibco 35050-061) and 4.5 µg/mL gentamicin (Gibco 15710-064). Cells were grown to confluency and passaged using trypsin-EDTA (0.05%) (Corning, 25-053-Cl) at least once before use in IP experiments.

VA4 treatment

Cultured cells were treated with 10 µM VA4 or 0.04% DMSO for vehicle control. For IP experiments, HEK 293TN cells were treated with VA4 12 hours after transfection, or 48 hours before protein collection. For immunoblot experiments, astrocytes were treated with VA4 for 48 hours before protein collection. Astrocytes on transwells used in neurite outgrowth studies were treated with VA4 1, 3 and 5 days before pairing with neurons at DIV 1. The VA4 was included in the transwell system and added again 48 hours later, on DIV 3.

Neurite Outgrowth Analyses

To seed the astrocytes onto the transwells, confluent, vehicle or VA4-treated WT astrocytes were passaged and seeded onto transwell inserts (6.5 mm) with a membrane pore size of 1.0 µm (Grenier Bio-One 665610) in glial MEM 48 hours prior to pairing with the neurons. The day the neurons were cultured the astrocytes in transwells were switched into supplemented neurobasal medium. On neuron DIV 1, the inserts were placed over the neurons on coverslips of a 12-well plate and the neurons received a half medium change with astrocyte-conditioned medium. The cell pairs were incubated for 96 hours and coverslips with neurons were collected for analysis of neurite outgrowth.

Coverslips of neurons from the transwell co-cultures were washed three times with PBS, followed by fixation with 4% paraformaldehyde and 4% sucrose in PBS for 5 min. After three washes with PBS, the cells were permeabilized with 0.25% Triton X-100 in PBS and blocked with PBS containing 5% BSA and 0.3 M glycine. Rabbit anti-MAP2 (Cell Signaling #8707S) was diluted in blocking buffer (1:200) and incubated overnight on the coverslips. The next day, the coverslips were washed three times and incubated in Alexa Fluor 594 donkey anti-rabbit

(Invitrogen A21207) for 1 h. Coverslips were then counterstained with Hoechst 33342 (1:10,000) and mounted using Fluoro-gel in TES Buffer (Electron Microscopy Sciences, 17985-30). The slides were imaged using a Zeiss Observer D1 microscope with a 40x objective.

Ten to fifteen neurons per coverslip were imaged for each condition. Images were processed by Image J Fiji using the Simple Neurite Tracer plugin. Neurites were traced using a scale of 6.7 pixel/µm. For the max neurite length studies, the longest neurite of each neuron was recorded.

Constructs

V5-tagged human TG2 in pcDNA and in the lentiviral vector FigB have been described previously (Gundemir et al. 2013, Ji et al. 2018). The FLAG-tagged Zbtb7a construct was purchased from Origene (RC222759).

Immunoblotting

Protein samples were resolved on 12% SDS-PAGE gels and proteins transferred to a nitrocellulose or PVDF membrane. Membranes were blocked in 5% milk in Tris-Buffered Saline with Tween20 (TBS-T) (20 mM Tris base, 137 mM NaCl, 0.05% Tween20) for 1 hour at room temperature. After blocking, primary antibodies against FLAG tag (CST 8146S), V5 tag (CST 13202S), GAPDH (Proteintech 60004-1-Ig), acetylated histone H3 K9 (CST 9649S) or beta tubulin (rabbit polyclonal antibody, Proteintech 10094-1-AP) were added to the blots in blocking buffer and incubated at 4℃ overnight. The next day blots were washed with TBS-T and incubated for one hr at room temperature with HRP-conjugated secondary antibody. The blots were washed with TBS-T before being visualized with an enhanced chemiluminescence reaction. ImageJ was used to quantify the intensity of each band, and all values were normalized to GAPDH or beta tubulin levels.

Co-immunoprecipitation

For immunoprecipitation (IP), HEK293TN were transfected with V5-TG2 and FLAG-Zbtb7a constructs using PolyJet transfection reagent (Signagen SL100688) following the manufacturer's protocol. The cells were treated with VA4 12 hours after transfection and collected 48 hours after VA4 treatment. The cells were lysed and collected in IP lysis buffer (150mM NaCl, 50 mM Tris-HCl, 1 mM EDTA, 1 mM EGTA, 0.5% NP-40 in PBS). Protein concentrations were measured using a BCA assay. A 300 µg aliquot of lysate was immunoprecipitated with 4 µL of rabbit anti-V5 tag antibody (CST 13202S). After addition of primary antibody, the samples were incubated on a rotator at 4 °C overnight. IgG control samples were incubated with an equivalent amount of normal rabbit (Millipore 12-370) IgG antibody. After 18 hours, 30 µL of Pierce protein A/G magnetic agarose, (Thermo Scientific 78609) washed in IP wash buffer (2mM EDTA, 0.1% NP-40 in PBS) and blocked in 1% BSA in PBS, were added. After a 4 hour incubation, rotating at 4 °C, the samples were thoroughly washed in IP wash buffer and then in IP lysis buffer. After washing, beads were incubated in 30 µL of 2.5x SDS in IP lysis buffer for 10 min at 100 °C. Samples were then immunoblotted as described above. For quantification, ImageJ was used to measure the intensity of FLAG and V5 bands in each lane and the FLAG signal was normalized to that of V5.

Sholl Analysis

Neurite outgrowth images were imported into Image J Fiji for Sholl analysis using SNT, which is toolbox for tracing and analyzing neuronal morphologies. For the analysis, images were converted to 8-bit, thresholded, made binary and skeletonized. A point was marked at the center of the soma and Sholl analysis was run using SNT. Sholl radii were set using the Image J default unit in increments of 5 and converted to microns using the 6.7 pixel/µm scale after analysis.

Statistical Analysis

GraphPad Prism 10 was used to report the raw data and perform statistical analysis. The mean values and standard error of the mean were calculated for each group. For significance testing, an unpaired *t*-test was used in Figures 2-4 and a one-way ANOVA in Figure 1, and levels of significance were set at *$p < 0.05$, **$p < 0.01$, ***$p < 0.001$, ****$p < 0.0001$. All statistical analysis information for each figure is shown in Table S1.

Acknowledgments: The authors would like to thank Joel Rodwell-Bullock for his assistance. This work was supported by NIH grant R21NS119673.

Author Contributions: Conceptualization, G.V.W.J., J.E., T.D.; Experimentation: J.E., T.D., M.H.; Data Analysis, G.V.W.J., J.E., T.D., M.H.; Manuscript preparation, Review and Editing, G.V.W.J., J.E., T.D., M.H., J.W.K.; Funding Acquisition, G.V.W.J. All authors have read and agreed to the published version of the manuscript.

Institutional Review Board Statement: The study was conducted in accordance with guidelines established by the University of Rochester Committee on Animal Resources (UCAR protocol #2007023E/R).

Conflicts of Interest: The authors declare no conflict of interest.

References

Akimov, S. S. and Belkin, A. M. (2001) Cell-surface transglutaminase promotes fibronectin assembly via interaction with the gelatin-binding domain of fibronectin: a role in TGFbeta-dependent matrix deposition. *J Cell Sci,* **114,** 2989-3000.

Anderson, M. A., Ao, Y. and Sofroniew, M. V. (2014) Heterogeneity of reactive astrocytes. *Neurosci Lett,* **565,** 23-29.

Barres, B. A. (2008) The mystery and magic of glia: a perspective on their roles in health and disease. *Neuron,* **60,** 430-440.

Basso, M. and Ratan, R. R. (2013) Transglutaminase is a therapeutic target for oxidative stress, excitotoxicity and stroke: a new epigenetic kid on the CNS block. *J Cereb Blood Flow Metab,* **33,** 809-818.

Begg, G. E., Carrington, L., Stokes, P. H., Matthews, J. M., Wouters, M. A., Husain, A., Lorand, L., Iismaa, S. E. and Graham, R. M. (2006) Mechanism of allosteric regulation of transglutaminase 2 by GTP. *Proc Natl Acad Sci U S A,* **103,** 19683-19688.

Burda, J. E., O'Shea, T. M., Ao, Y. et al. (2022) Divergent transcriptional regulation of astrocyte reactivity across disorders. *Nature,* **606,** 557-564.

Chen, J. S. and Mehta, K. (1999) Tissue transglutaminase: an enzyme with a split personality. *Int J Biochem Cell Biol,* **31,** 817-836.

Choi, W. I., Jeon, B. N., Yun, C. O., Kim, P. H., Kim, S. E., Choi, K. Y., Kim, S. H. and Hur, M. W. (2009) Proto-oncogene FBI-1 represses transcription of p21CIP1 by inhibition of transcription activation by p53 and Sp1. *J Biol Chem,* **284,** 12633-12644.

Chung, W. S., Allen, N. J. and Eroglu, C. (2015) Astrocytes Control Synapse Formation, Function, and Elimination. *Cold Spring Harb Perspect Biol,* **7,** a020370.

Colak, G. and Johnson, G. V. (2012) Complete transglutaminase 2 ablation results in reduced stroke volumes and astrocytes that exhibit increased survival in response to ischemia. *Neurobiol Dis,* **45,** 1042-1050.

Colak, G., Keillor, J. W. and Johnson, G. V. (2011) Cytosolic guanine nucledotide binding deficient form of transglutaminase 2 (R580a) potentiates cell death in oxygen glucose deprivation. *PLoS One,* **6,** e16665.

Davies, S. J., Fitch, M. T., Memberg, S. P., Hall, A. K., Raisman, G. and Silver, J. (1997) Regeneration of adult axons in white matter tracts of the central nervous system. *Nature,* **390,** 680-683.

Delgado, T. and Johnson, G. V. W. (2024) Transglutaminase 2 in neurological conditions. In: *Transglutaminase Fundamentals and Applications*, (B. K. Simpson and Y. Zhang eds.), pp. 107-130. Elsevier, Academic Press.

Eckert, R. L., Kaartinen, M. T., Nurminskaya, M., Belkin, A. M., Colak, G., Johnson, G. V. and Mehta, K. (2014) Transglutaminase regulation of cell function. *Physiol Rev,* **94,** 383-417.

Elahi, A., Emerson, J., Rudlong, J., Keillor, J. W., Salois, G., Visca, A., Girardi, P., Johnson, G. V. W. and Proschel, C. (2021) Deletion or Inhibition of Astrocytic Transglutaminase 2 Promotes Functional Recovery after Spinal Cord Injury. *Cells,* **10**.

Emerson, J., Delgado, T., Girardi, P. and Johnson, G. V. W. (2023) Deletion of Transglutaminase 2 from Mouse Astrocytes Significantly Improves Their Ability to Promote Neurite Outgrowth on an Inhibitory Matrix. *Int J Mol Sci,* **24**.

Escartin, C., Galea, E., Lakatos, A. et al. (2021) Reactive astrocyte nomenclature, definitions, and future directions. *Nat Neurosci,* **24,** 312-325.

Espitia Pinzon, N., Breve, J. J. P., Bol, J., Drukarch, B., Baron, W. and van Dam, A. M. (2017) Tissue transglutaminase in astrocytes is enhanced by inflammatory mediators and is involved in the formation of fibronectin fibril-like structures. *J Neuroinflammation,* **14,** 260.

Farrelly, L. A., Thompson, R. E., Zhao, S. et al. (2019) Histone serotonylation is a permissive modification that enhances TFIID binding to H3K4me3. *Nature,* **567,** 535-539.
Feola, J., Barton, A., Akbar, A., Keillor, J. and Johnson, G. V. W. (2017) Transglutaminase 2 modulation of NF-kappaB signaling in astrocytes is independent of its ability to mediate astrocytic viability in ischemic injury. *Brain Res,* **1668,** 1-11.
Filiano, A. J., Bailey, C. D., Tucholski, J., Gundemir, S. and Johnson, G. V. (2008) Transglutaminase 2 protects against ischemic insult, interacts with HIF1beta, and attenuates HIF1 signaling. *FASEB J,* **22,** 2662-2675.
Filiano, A. J., Tucholski, J., Dolan, P. J., Colak, G. and Johnson, G. V. (2010) Transglutaminase 2 protects against ischemic stroke. *Neurobiol Dis,* **39,** 334-343.
Gates, L. A., Shi, J., Rohira, A. D. et al. (2017) Acetylation on histone H3 lysine 9 mediates a switch from transcription initiation to elongation. *J Biol Chem,* **292,** 14456-14472.
Griffin, M., Casadio, R. and Bergamini, C. M. (2002) Transglutaminases: nature's biological glues. *Biochem J,* **368,** 377-396.
Gundemir, S., Colak, G., Feola, J., Blouin, R. and Johnson, G. V. (2013) Transglutaminase 2 facilitates or ameliorates HIF signaling and ischemic cell death depending on its conformation and localization. *Biochim Biophys Acta,* **1833,** 1-10.
Gundemir, S., Colak, G., Tucholski, J. and Johnson, G. V. (2012) Transglutaminase 2: a molecular Swiss army knife. *Biochim Biophys Acta,* **1823,** 406-419.
Gundemir, S. and Johnson, G. V. (2009) Intracellular localization and conformational state of transglutaminase 2: implications for cell death. *PLoS One,* **4,** e6123.
Gundemir, S., Monteagudo, A., Akbar, A., Keillor, J. W. and Johnson, G. V. W. (2017) The complex role of transglutaminase 2 in glioblastoma proliferation. *Neuro-Oncology,* **19,** 208-218.
Guttenplan, K. A., Weigel, M. K., Prakash, P. et al. (2021) Neurotoxic reactive astrocytes induce cell death via saturated lipids. *Nature,* **599,** 102-107.
Icardi, L., Mori, R., Gesellchen, V. et al. (2012) The Sin3a repressor complex is a master regulator of STAT transcriptional activity. *Proc Natl Acad Sci U S A,* **109,** 12058-12063.
Ientile, R., Caccamo, D., Marciano, M. C., Curro, M., Mannucci, C., Campisi, A. and Calapai, G. (2004) Transglutaminase activity and transglutaminase mRNA transcripts in gerbil brain ischemia. *Neurosci Lett,* **363,** 173-177.
Ientile, R., Curro, M. and Caccamo, D. (2015) Transglutaminase 2 and neuroinflammation. *Amino Acids,* **47,** 19-26.
Ji, C., Tang, M., Harrison, J., Paciorkowski, A. and Johnson, G. V. W. (2018) Nuclear transglutaminase 2 directly regulates expression of cathepsin S in rat cortical neurons. *Eur J Neurosci,* **48,** 3043-3051.
Kadamb, R., Mittal, S., Bansal, N., Batra, H. and Saluja, D. (2013) Sin3: insight into its transcription regulatory functions. *Eur J Cell Biol,* **92,** 237-246.
Keillor, J. W. and Johnson, G. V. W. (2021) Transglutaminase 2 as a therapeutic target for neurological conditions. *Expert Opin Ther Targets,* **25,** 721-731.
Kim, H. J., Lee, J. H., Cho, S. Y., Jeon, J. H. and Kim, I. G. (2021) Transglutaminase 2 mediates transcriptional regulation through BAF250a polyamination. *Genes Genomics,* **43,** 333-342.
Laudes, M., Bilkovski, R., Oberhauser, F., Droste, A., Gomolka, M., Leeser, U., Udelhoven, M. and Krone, W. (2008) Transcription factor FBI-1 acts as a dual regulator in adipogenesis by coordinated regulation of cyclin-A and E2F-4. *J Mol Med (Berl),* **86,** 597-608.
Lepack, A. E., Werner, C. T., Stewart, A. F. et al. (2020) Dopaminylation of histone H3 in ventral tegmental area regulates cocaine seeking. *Science,* **368,** 197-201.
Lesort, M., Attanavanich, K., Zhang, J. and Johnson, G. V. (1998) Distinct nuclear localization and activity of tissue transglutaminase. *J Biol Chem,* **273,** 11991-11994.

Liddelow, S. A., Guttenplan, K. A., Clarke, L. E. et al. (2017) Neurotoxic reactive astrocytes are induced by activated microglia. *Nature,* **541,** 481-487.
Linnerbauer, M. and Rothhammer, V. (2020) Protective Functions of Reactive Astrocytes Following Central Nervous System Insult. *Front Immunol,* **11,** 573256.
Liu, S., Cerione, R. A. and Clardy, J. (2002) Structural basis for the guanine nucleotide-binding activity of tissue transglutaminase and its regulation of transamidation activity. *Proc Natl Acad Sci U S A,* **99,** 2743-2747.
McConoughey, S. J., Basso, M., Niatsetskaya, Z. V. et al. (2010) Inhibition of transglutaminase 2 mitigates transcriptional dysregulation in models of Huntington disease. *EMBO Mol Med,* **2,** 349-370.
Milakovic, T., Tucholski, J., McCoy, E. and Johnson, G. V. (2004) Intracellular localization and activity state of tissue transglutaminase differentially impacts cell death. *J Biol Chem,* **279,** 8715-8722.
Mironov, G. G., Clouthier, C. M., Akbar, A., Keillor, J. W. and Berezovski, M. V. (2016) Simultaneous analysis of enzyme structure and activity by kinetic capillary electrophoresis-MS. *Nat Chem Biol,* **12,** 918-922.
Monteagudo, A., Feola, J., Natola, H., Ji, C., Proschel, C. and Johnson, G. V. W. (2018) Depletion of astrocytic transglutaminase 2 improves injury outcomes. *Mol Cell Neurosci,* **92,** 128-136.
Pinkas, D. M., Strop, P., Brunger, A. T. and Khosla, C. (2007) Transglutaminase 2 undergoes a large conformational change upon activation. *Plos Biol,* **5,** e327.
Pittol, J. M. R., Oruba, A., Mittler, G., Saccani, S. and van Essen, D. (2018) Zbtb7a is a transducer for the control of promoter accessibility by NF-kappa B and multiple other transcription factors. *Plos Biol,* **16**.
Quinn, B. R., Yunes-Medina, L. and Johnson, G. V. W. (2018) Transglutaminase 2: Friend or foe? The discordant role in neurons and astrocytes. *J Neurosci Res,* **96,** 1150-1158.
Rossin, F., Ciccosanti, F., D'Eletto, M., Occhigrossi, L., Fimia, G. M. and Piacentini, M. (2023) Type 2 transglutaminase in the nucleus: the new epigenetic face of a cytoplasmic enzyme. *Cell Mol Life Sci,* **80,** 52.
Rroji, O., Kumar, A., Karuppagounder, S. S. and Ratan, R. R. (2021) Epigenetic regulators of neuronal ferroptosis identify novel therapeutics for neurological diseases: HDACs, transglutaminases, and HIF prolyl hydroxylases. *Neurobiol Dis,* **147,** 105145.
Smith, G. M. and Strunz, C. (2005) Growth factor and cytokine regulation of chondroitin sulfate proteoglycans by astrocytes. *Glia,* **52,** 209-218.
Sofroniew, M. V. and Vinters, H. V. (2010) Astrocytes: biology and pathology. *Acta Neuropathol,* **119,** 7-35.
Tatsukawa, H., Furutani, Y., Hitomi, K. and Kojima, S. (2016) Transglutaminase 2 has opposing roles in the regulation of cellular functions as well as cell growth and death. *Cell Death Dis,* **7,** e2244.
Tiana, M., Acosta-Iborra, B., Puente-Santamaria, L. et al. (2018) The SIN3A histone deacetylase complex is required for a complete transcriptional response to hypoxia. *Nucleic Acids Res,* **46,** 120-133.
van Strien, M. E., Breve, J. J., Fratantoni, S., Schreurs, M. W., Bol, J. G., Jongenelen, C. A., Drukarch, B. and van Dam, A. M. (2011a) Astrocyte-derived tissue transglutaminase interacts with fibronectin: a role in astrocyte adhesion and migration? *PLoS One,* **6,** e25037.
van Strien, M. E., Drukarch, B., Bol, J. G., van der Valk, P., van Horssen, J., Gerritsen, W. H., Breve, J. J. and van Dam, A. M. (2011b) Appearance of tissue transglutaminase in astrocytes in multiple sclerosis lesions: a role in cell adhesion and migration? *Brain Pathol,* **21,** 44-54.

Yiu, G. and He, Z. (2006) Glial inhibition of CNS axon regeneration. *Nat Rev Neurosci,* **7,** 617-627.

Yunes-Medina, L., Feola, J. and Johnson, G. V. W. (2017) Subcellular localization patterns of transglutaminase 2 in astrocytes and neurons are differentially altered by hypoxia. *Neuroreport,* **28,** 1208-1214.

Figure Legends

Figure 1. VA4 inhibition of TG2 facilitates the ability of WT astrocytes to promote neurite outgrowth on a CSPG growth-inhibitory matrix. (a) Schematic of neurite outgrowth experimental paradigm including VA4 treatment. Created with BioRender.com. (b) Representative images of MAP2-staining of neurons without paired astrocytes, neurons paired with vehicle (DMSO)-treated astrocytes, or neurons paired with VA4-treated astrocytes (scale bar = 20 µm). (c) Quantification of length of longest neurite for neuron experimental groups on CSPG matrix (n= 86-111 neurons per group from two biological replicates, one-way ANOVA ****$p < 0.0001$).

Figure 2. Irreversible inhibition of TG2 with the drug VA4 reduces interaction between TG2 and Zbtb7a. (a) Input controls of V5-TG2 and FLAG-Zbtb7a transfected into HEK 293TN cells treated with VA4 or vehicle control (DMSO). (b) Immunoprecipitation of V5-TG2 pulls down less FLAG-Zbtb7a in cell lysates that were treated with VA4. In (a) and (b) the position at which molecular weight markers (kDa) migrated is indicated at the left of the immunoblots. (c) Quantification of the amount of FLAG-Zbtb7a pulled down normalized to the amount of V5-TG2 immunoprecipitated. Treatment of cells with VA4 resulted in a significant reduction in the Zbtb7a co-immunoprecipitated with TG2 compared to DMSO control (n=5 samples per condition from 4 independent biological replicates, unpaired t-test ****$p < 0.0001$).

Figure 3. Histone acetylation of H3K9 is significantly greater in TG2-/- astrocytes compared to WT astrocytes. (a) Representative western blot of WT and TG2-/- astrocyte lysates probed for Histone H3 acetylated at lysine residue 9 (H3K9ac). The position at which molecular weight markers (kDa) migrated is indicated at the left of the immunoblots. (b) Quantification of H3K9ac levels in WT and TG2-/- astrocytes. TG2-/- astrocytes showed significantly great acetylation of H3K9 than WT astrocytes (~60%) (n=1-4 samples per condition from 4 independent biological replicates, unpaired t-test **$p < 0.01$).

Figure 4. Histone acetylation of H3K9 is significantly greater in WT astrocytes treated with VA4 compared to WT astrocytes treated with DMSO vehicle control. (a) Western blot of 10 µM VA4 and vehicle control treated WT astrocyte lysates probed for H3K9ac. The position at which molecular weight markers (kDa) migrated is indicated at the left of the immunoblots. (b) Quantification of H3K9ac levels in VA4 treated WT astrocytes showed significantly great acetylation than vehicle control treated WT astrocytes (~65%) (n=3 samples per condition from 2 independent biological replicates, unpaired t-test *$p < 0.01$).

Figure 5. Proposed mechanism by which TG2 modulates the neuroprotective phenotype of reactive astrocytes. In stressed astrocytes TG2 is able to move in and out of the nucleus. When in the nucleus TG2 interacts with Zbtb7a and Sin3a, resulting in increased HDAC activity and neurosupportive gene repression. If TG2 is deleted from the astrocytes, or the astrocytes are treated with VA4 the recruitment of Zbtb7a/Sin3a/HDAC to the DNA is diminished resulting in de-repression of neurosupportive genes leading to a more neurosupportive phenotype. The “?” indicates that the effect of VA4 treatment on the nuclear/cytosolic localization of TG2 is unclear. Created with BioRender.com.

Figure 1

(a)

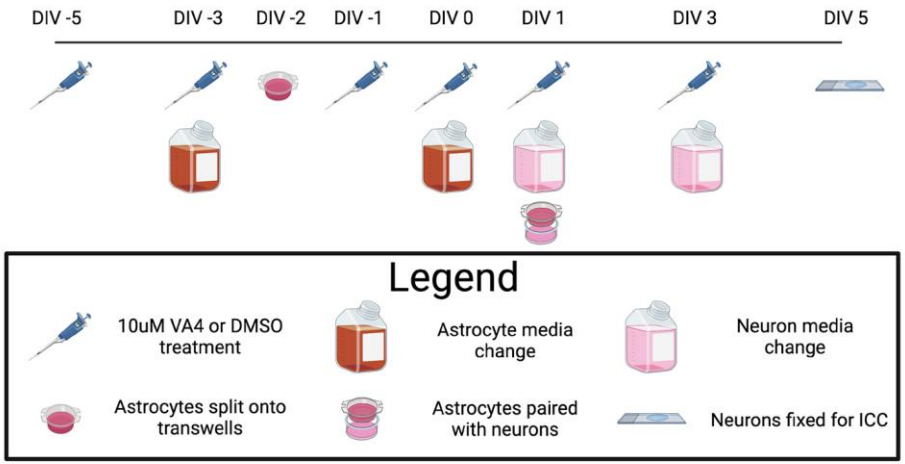
DIV -5
DIV -3
DIV -2
DIV -1
DIV 0
DIV 1
DIV 3
DIV 5
Legend
10uM VA4 or DMSO treatment
Astrocyte media change
Neuron media change
Astrocytes split onto transwells
Astrocytes paired with neurons
Neurons fixed for ICC

(b)

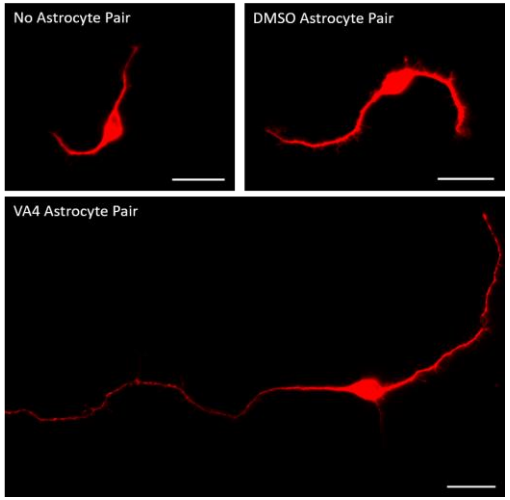
No Astrocyte Pair
DMSO Astrocyte Pair
VA4 Astrocyte Pair

(c)

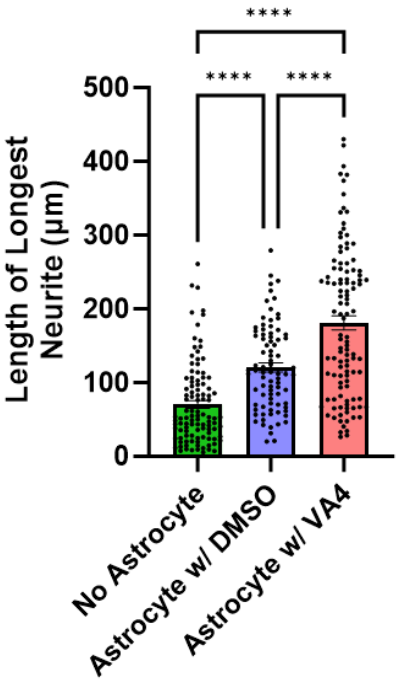
****
****
****
Length of Longest Neurite (µm)
500
400
300
200
100
0
No Astrocyte
Astrocyte w/ DMSO
Astrocyte w/ VA4

Figure 2

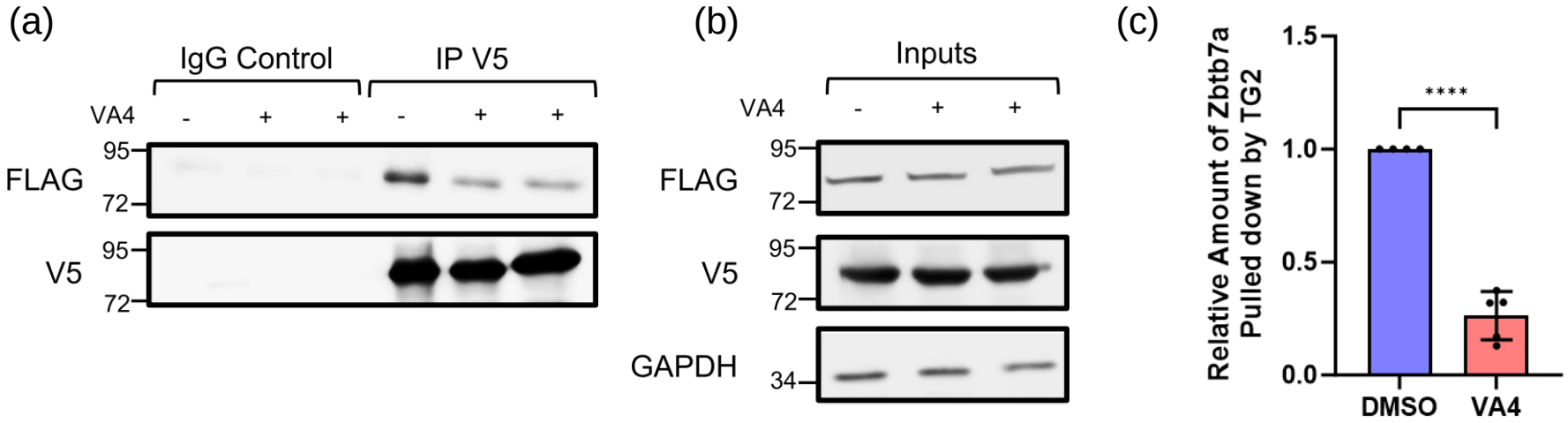
(a)
IgG Control
IP V5
VA4
- + + - + +
FLAG
95
72
V5
95
72
(b)
Inputs
VA4
- + +
FLAG
95
72
V5
95
72
GAPDH
34
(c)
Relative Amount of Zbtb7a Pulled down by TG2
1.5
1.0
0.5
0.0
****
DMSO
VA4

Figure 3

(a)
WT
TG2-/-
H3K9ac
17
β Tubulin
55
(b)
Relative Histone Acetylation
2.5
2.0
1.5
1.0
0.5
0.0
**
WT
TG2-/-

Figure 4

(a)

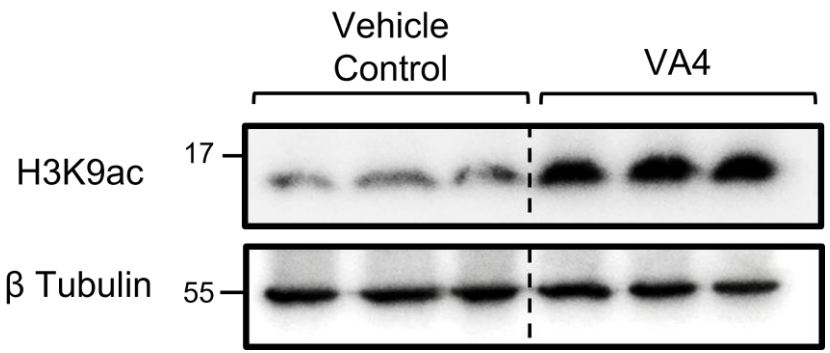
Vehicle
Control
VA4
H3K9ac
17
β Tubulin
55

(b)

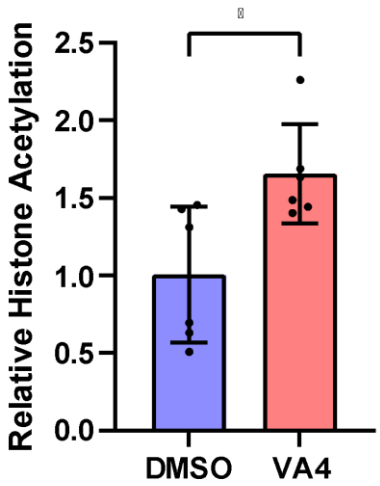
Relative Histone Acetylation
2.5
2.0
1.5
1.0
0.5
0.0
DMSO
VA4

Figure 5

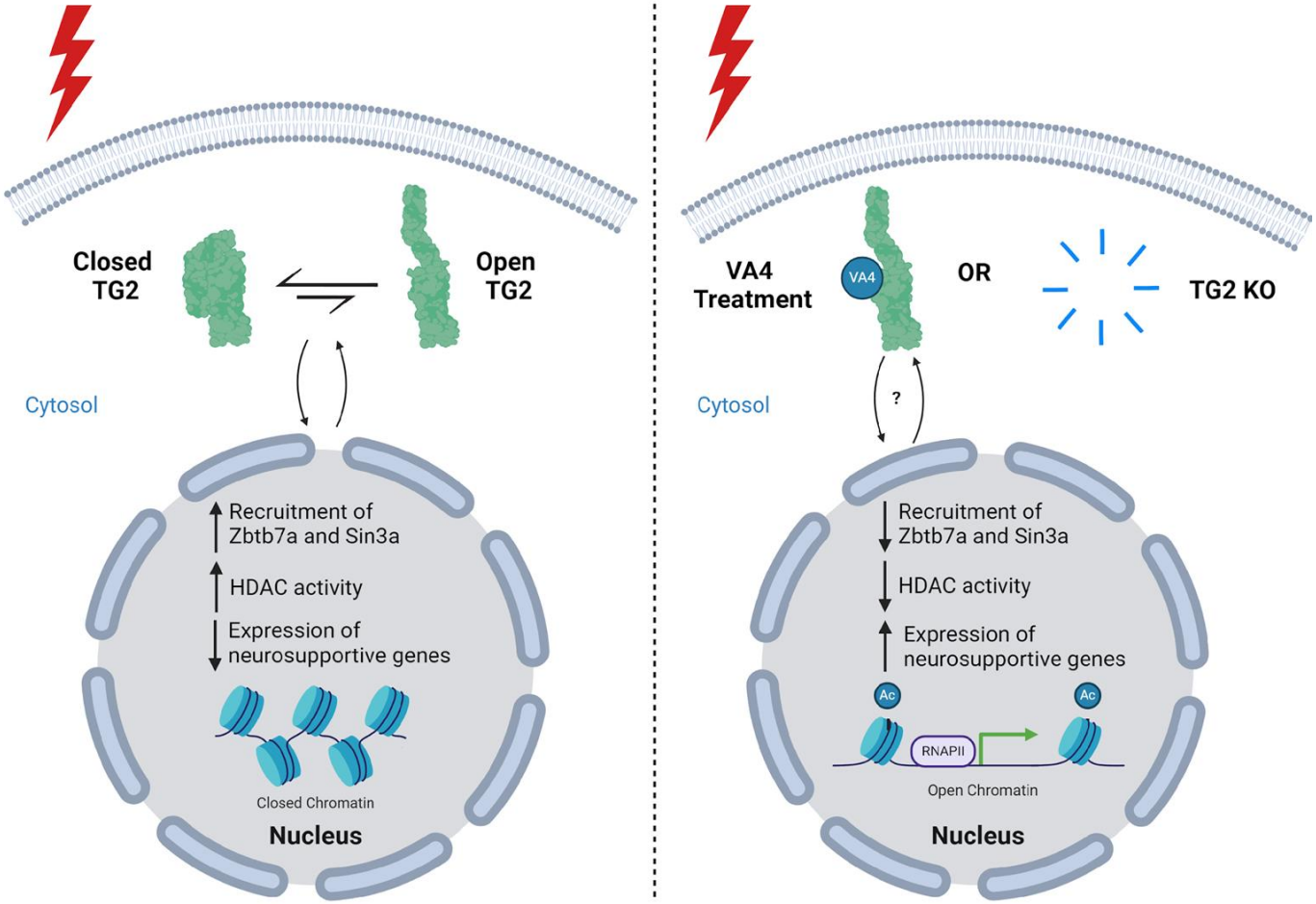
Closed
TG2
Open
TG2
Cytosol
Recruitment of
Zbtb7a and Sin3a
HDAC activity
Expression of
neurosupportive genes
Closed Chromatin
Nucleus
VA4
Treatment
VA4
OR
TG2 KO
Cytosol
?
Recruitment of
Zbtb7a and Sin3a
HDAC activity
Expression of
neurosupportive genes
Ac
Ac
RNAPII
Open Chromatin
Nucleus

Table S1

	Test	Sided	Multiple Comparison Correction?	DF	Test Statistic	p-value
Figure 1c	1 way ANOVA	one	Tukey Correction	2, 300	F=58.33	p<0.0001
Figure 2c	T test	two	N/A	7	t=13.61	p<0.0001
Figure 3b	T test	two	N/A	25	t=3.525	p=0.0017
Figure 4b	T test	two	N/A	3	t=7.528	p=0.0049
Figure S1	2 way ANOVA	one	Tukey Correction	12, 4, 3, 643	F (12, 643) = 8.257 F(4, 643) = 107.9 F (3,643) = 48.69	p<0.0001 p<0.0001 p<0.0001
Figure S2	2 way ANOVA	one	Tukey Correction	35, 3, 105	F (35, 105) =1.306 F (3, 105)= 63.41	p=0.1512 p<0.0001

For all statistical tests significance values were pre-determined to be *p<0.05, **p<0.01, ***p<0.001, ****p< 0.0001.

Supplemental Figures

Figure S1

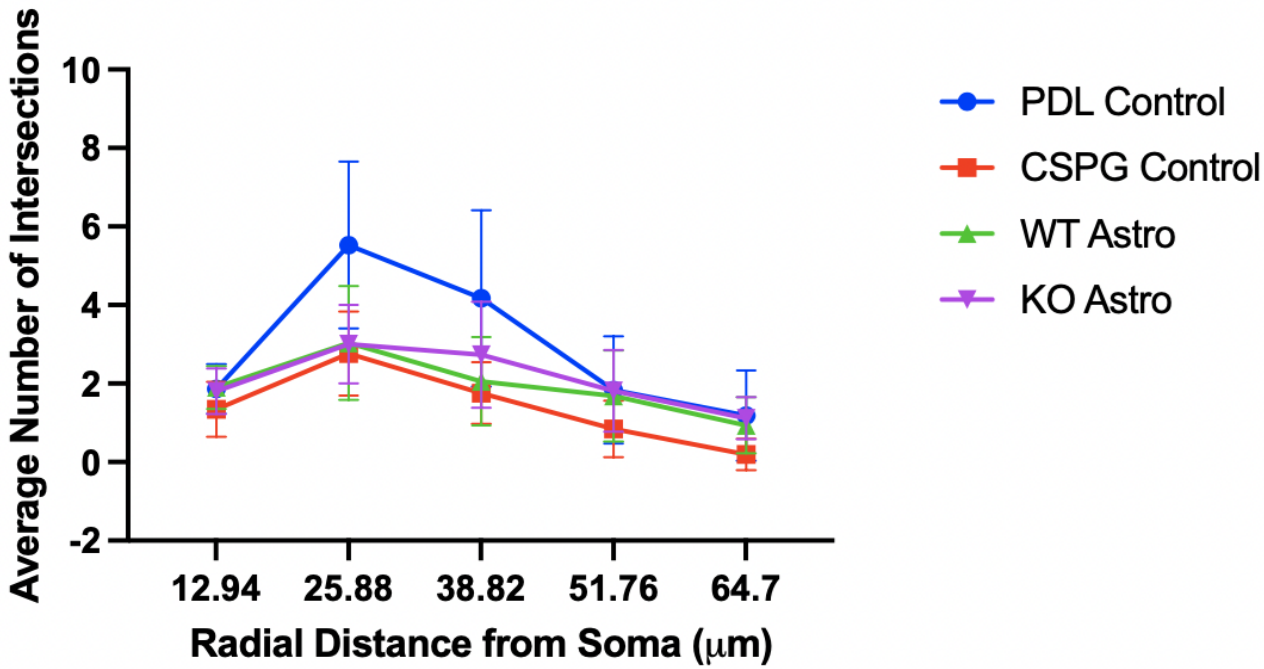

WT and TG2-/- astrocytes do not recover neuronal complexity when grown on an inhibitory CSPG matrix. (a) Summary data of Sholl analysis of neurite outgrowth images from (Emerson et al., 2023). Blue symbols/line show neurite branching on a control matrix (PDL Control). Red symbols/line shown neurite branching on an inhibitory matrix (CSPG Control). Green symbols/line show branching on CSPGs in the presence of wild type astrocytes (WT Astro) and the purple symbol/line shows branching in the presence of TG2-/- astrocytes (KO Astro) Plot shows average number of intersections with each Scholl radii and the standard deviation (n=33-42 neurons per condition from 2 biological replicates, Two-way ANOVA).

Figure S2

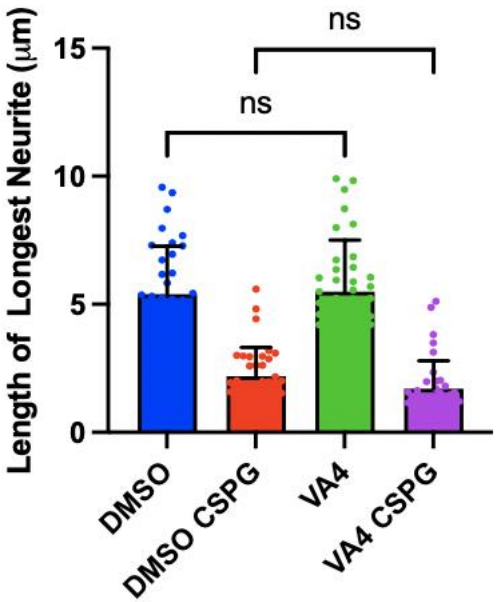

VA4 treatment of neurons does not affect neurite outgrowth on poly D lysine or CSPG matrices. Neurons were directly treated with DMSO (control) or 10 μM VA4 for 4 days prior to quantification of neurite length on PDL or CSPG matrices. (n=36 neurons per condition from 1 biological replicate, Two-way ANOVA).